Nonadiabatic effects in the dynamics of atoms confined in a cylindric time-orbiting-potential magnetic trap

Roberto Franzosi*

INFN Sezione di Pisa and INFM UdR di Pisa, Dipartimento di Fisica E. Fermi, Università di Pisa, Via Buonarroti 2, I-56127 Pisa, Italy

Bruno Zambon[†] and Ennio Arimondo

INFM UdR di Pisa, Dipartimento di Fisica E. Fermi, Università di Pisa, Via Buonarroti 2, I-56127 Pisa, Italy

In a time-orbiting-potential magnetic trap the neutral atoms are confined by means of an inhomogeneous magnetic field superimposed onto an uniform rotating one. We perform an analytic study of the atomic motion by taking into account the nonadiabatic effects arising from the spin dynamics about the local magnetic field. Geometric like magnetic fields determined by Berry's phase appear within the quantum description. Application of the time-dependent variational principle on the original quantum equation leads to a set of dynamical evolution equations for the quantum average value of the position operator and spin variables. Within this approximation we derive the quantum-mechanical ground-state configuration matching the classical adiabatic solution and perform some numerical simulations.

I. INTRODUCTION

The difficulty of analyzing a complex physical system is greatly reduced when one is able to identify a certain number of different time scales present in the system dynamical evolution. Thus, a series of approximations, generically termed adiabatic approximations, can successfully be carried out. The very simple basic idea is that of dealing first with the motion of the fast variables, keeping the slow ones fixed but arbitrary, and then to complete the analysis of the entire system by allowing a variation of the previously fixed coordinates. The quantum adiabatic theorem and the molecular Born-Oppenheimer approximation are well-known examples of this approach, with its origins in the early days of quantum mechanics. The quantum-adiabatic theorem dictates that a system prepared in an eigenstate of its Hamiltonian will remain in the corresponding eigenstate as the Hamiltonian is varied slowly enough. If the Hamiltonian returns to its original form, the system assumes the original eigenstate multiplied by an appropriate dynamical phase factor related to the instantaneous eigenvalue of the Hamiltonian. Berry made the interesting observation that in addition to the dynamical phase factor produced by the eigenvalue time evolution, the wave-function acquires an additional phase contribution [1]. This additional contribution, the geometric phase, depends only on the path traveled by the system in the space of external parameters.

A canonical example for a system where this behavior occurs is that of a neutral particle carrying a magnetic moment and moving in an inhomogeneous magnetic field. Here, the fast variable is the transverse magnetic moment and the slow variable is the atomic position and momentum [2]. If the magnetic field varies slowly enough in space, the effective Hamiltonian governing the dynamics of the slow external variables contains an induced gauge potential, the so-called geometric potential. It also depends on the component of the magnetic moment in the direction of the magnetic field which is an adiabatic invariant approximatively conserved. In the classical limit the gauge geometric fields acting on the neutral particle with a magnetic moment have been studied by Aharonov and Stern [3]; they found that the atom experiences geometric Lorentz-type and electric-type forces [4]. The magnitudes of these forces do not depend on the amplitude of the magnetic field, but only on its local orientation.

In order to treat the nonadiabatic corrections improved Born-Oppenheimer methods were introduced for the case of arbitrary spin values [5]. Later the nonadiabatic terms modifying the atomic motion were studied by several authors in the context of magnetic structures guiding or confining very cold atoms [6–9]. The nonadiabatic corrections produce spin-flip transitions, leading to atomic loss from the magnetic configurations, and also they modify the atomic motion. Yukalov [10] considered nonadiabatic dynamics of trapped atoms by applying an accurate method for solving nonlinear systems of differential equations. High-order post-adiabatic corrections, leading to geometric electromagnetism potentials, have been investigated for the elegant configuration of an atom orbiting around a straight current-carrying wire [11]. For verification of Berry's phase and its consequences a natural question is whether one can observe the direct modification of the atomic motion in the classical limit for the induced gauge potentials. Measurements of the motion of a rubidium Bose-Einstein condensate in a time-orbiting-potential (TOP) magnetic trap represent quite a strong indication for the existence of these geometric forces [12–14]. Those observations were analyzed through a classical description for the condensate center-of-mass motion and for the atomic magnetic moment.

In the present paper we perform an analytic study of the atomic quantum dynamics within TOP magnetic traps. We

---

*Electronic address: Roberto.Franzosi@df.unipi.it

†Electronic address: Bruno.Zambon@df.unipi.it

take into account the nonadiabatic effects arising from the dynamics of the spin orientation around the local magnetic field. Within a pure quantum description, the geometric magnetic fields appear as a consequence of the presence of inhomogeneous magnetic fields. In this context spinors quantities can be introduced to describe the atomic spin states, as done by Ho and Shenoy [6] for Berry's phase in atomic condensates in magnetic traps. By means of the time-dependent variation principle (TDVP) [15] and by taking advantage of the time scale separation between slow and fast variables, we derive an effective atomic dynamics making the quantum description analytically tractable. Thus, the atomic motion results in the coupling of a quantum harmonic motion, governing the atomic scalar wave function, and an effective nonlinear spin dynamics. The harmonic Hamiltonian depends on time-varying parameters that, in turn, are linked to the spin state. Also the spin Hamiltonian parameters are time dependent, as they result from the atomic wave-function expectation values of the above geometric operators. Within this nonadiabatic approximation the ground-state configuration matches well the adiabatic solution. We also performed numerical simulations with these new equations. For the parameters suggested by the standard experimental setup we found that the adiabatic approximation is well suited. Nevertheless, by reducing the intensity of the bias field, nonadiabatic effects show up, because under these conditions the influence of the geometric fields is more relevant. A recent work [16] has examined theoretically the condensate micromotion, applying the adiabatic approximation and partially lifting the time-average approximation by a unitary transformation to a frame circularly translating at the frequency of the TOP magnetic field. That approach, neglecting spin precession effects leading to the breakdown of the adiabatic approximation, cannot be directly applied to the analysis of geometric forces.

Section II summarizes the classical analysis based on the adiabatic approximation and leading to the atomic micromotion. Section III reports a quantum analysis of the atomic motion within the adiabatic approximation by taking into account the lowest-frequency terms of the time-dependent potential. Within this approximation we recover the quantum counterpart of the classical micromotion. Section IV studies the quantum dynamics of atoms into TOP traps. In Sec. V, by means of the TDVP, we derive an effective dynamics for the atomic motion. Section VI reports numerical simulations for the dynamical regime of the atomic motion.

II. TOP TRAP

Bose-Einstein condensation in dilute atomic gas is created by trapping cold atoms in a magnetic trap of which the Ioffe-Pritchard (IP) and time-orbiting potentials are the most common ones. In a TOP trap the magnetic field, schematically represented in the inset of Fig. 1, is composed of a quadrupole (inhomogeneous) field and a rotating (time-dependent) bias field, B_0. The TOP trap, introduced in [17] for the very first experiments on Bose-Einstein condensation [18], is employed by a number of research groups producing Bose-Einstein condensates [19,21,20–23].
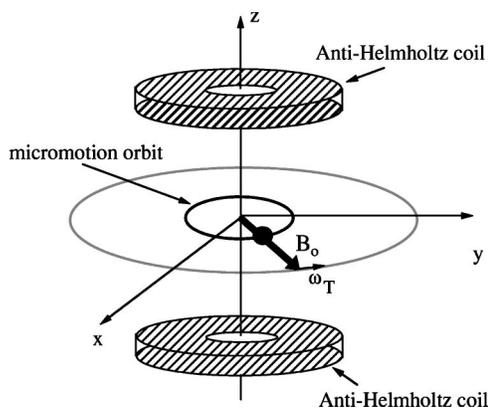
FIG. 1. Schematic representation of a cylindric TOP trap with the anti-Helmholtz coils producing a quadrupole field with vertical symmetry, the B_0 bias field rotating at angular frequency ω_T in the horizontal plane, and the atomic cloud (black sphere) following the micromotion orbit.

The single-particle Hamiltonian for the atoms inside a magnetic field configuration which characterizes the trap geometry is given by

$$H(t) = \frac{\mathbf{p}^2}{2m} + mgz - \frac{\mu}{s}\mathbf{s} \cdot \mathbf{B}(\mathbf{x},t), \quad (1)$$

where $\mathbf{s}$ are the spin operators of the $s=\hbar j$ representation, and the last term takes into account the magnetic interaction energy of an atom with magnetic moment $\mu\mathbf{s}/s$ and projection $\mu=-|\mu|$ along the magnetic field $\mathbf{B}$. We also adopt the representation $\mathbf{x}=x\hat{x}+y\hat{y}+z\hat{z}$ for the position vector. For a TOP trap the magnetic field is the superposition of a static quadrupole field and one rotating at the radio frequency (rf) ω_T:

$$\mathbf{B}(\mathbf{x},t) = \mathbf{b}(\mathbf{x}) + \mathbf{B}_t(t). \quad (2)$$

Its components are

$$\mathbf{b}(\boldsymbol{x}) = b_x x\hat{x} + b_y y\hat{y} + b_z z\hat{z} \quad (3)$$

and

$$\boldsymbol{B}_t(t) = B_0\cos(\omega_T t)\hat{x} + B_0\sin(\omega_T t)\hat{y}. \quad (4)$$

The magnetic field parameters define the specific type of TOP trap we are analyzing [24]. By supposing the rf field rotating in the horizontal x,y plane we define the TOP geometry of the traps operating at Boulder [17] and at Pisa [25]. In this work we analyze the dynamics of a cylindric TOP trap with

$$b_x = b_y = -b_z/2 = b. \quad (5)$$

For the usual TOP trap three different time scales exists: the fastest motion, given by the Larmor frequency ω_L and related to the spin precession around the local magnetic field; the magnetic bias field rotating frequency ω_T giving rise to time-dependent forces at the frequences $\omega_T, 2\omega_T, \ldots$, and a slower motion associated with the atom spatial motion given by the trap harmonic frequency ω_h. These time scales are in order of magnitude,—i.e., $\omega_h \ll \omega_T \ll \omega_L$—thus making possible the

adiabatic approximation. In the first place the fast spin precession around the local magnetic field allows us to consider atoms spin locked to the local magnetic field throughout the whole spatial motion. This leads to an adiabatic-time dependent potential $U = -(\mu/s)\mathbf{s} \cdot \mathbf{B}(\mathbf{x}, t) = |\mu| \cdot |\mathbf{B}(\mathbf{x}, t)|$. Second by averaging in time (over a period $2\pi/\omega_T$) this potential and by keeping only the slowest component gives rise to a harmonic potential spatially confining the condensate. The next order of approximation examines the fast variables (fast with respect to the harmonic dynamics at frequency ω_h) related to the time-dependent potential (at frequency ω_T). An exhaustive computation of this approximation is found in [26].

Gov and Shtrikman [27] have used the standard classical equations of the atomic motion of a magnetic moment within a TOP in which all the different time scales are present. In this context a steady periodic orbit can be found exactly without resorting to any approximation. This periodic solution corresponds to what it is known as the *atomic micromotion* [28] (see Fig. 1). As the atoms trace out the atomic micromotion orbit, the magnitude and direction of the local magnetic field change in space and time, with the magnetic moment of the atom precessing around the direction of the field. In fact, given the Hamiltonian of Eq. (1) a dynamical state $|\Psi\rangle$ satisfies the following center-of-mass equations of motion:

$$m\frac{d^2\mathbf{R}}{dt^2} = \frac{\mu}{s}\boldsymbol{\nabla}[\mathbf{S} \cdot \mathbf{b}(\mathbf{R})] - mg\hat{z},$$

$$\frac{d\mathbf{S}}{dt} = \frac{\mu}{s}\langle\Psi|\mathbf{s} \times \mathbf{B}(\mathbf{x}, t)|\Psi\rangle, \qquad (6)$$

where $\mathbf{R} = X\hat{x} + Y\hat{y} + Z\hat{z} = \langle\Psi|\mathbf{x}|\Psi\rangle$ is the expectation value of the center-of-mass position, and $\mathbf{S} = S_x\hat{x} + S_y\hat{y} + S_z\hat{z} = \langle\Psi|\mathbf{s}|\Psi\rangle$ is the expectation value of the atomic spin.

Thus we are led to a set of equations which are not closed. However, if the quantum mechanical wave function can be factorized, as to the lowest-order approximation, we may write $\langle\mathbf{s} \times \mathbf{B}(\mathbf{x}, t)\rangle = \langle\mathbf{s}\rangle \times \langle\mathbf{B}(\mathbf{x}, t)\rangle$ [29]. Within this approximation the above system of equations becomes closed and assumes the form

$$m\frac{d^2\mathbf{R}}{dt^2} = \frac{\mu}{s}\boldsymbol{\nabla}[\mathbf{S} \cdot \mathbf{b}(\mathbf{R})] - mg\hat{z},$$

$$\frac{d\mathbf{S}}{dt} = \frac{\mu}{s}\mathbf{S} \times \mathbf{B}(\mathbf{R}, t). \qquad (7)$$

The simplest periodic solutions generated by Eqs. (7) give a good estimate of the fast center-of-mass condensate dynamics,—i.e., the atomic micromotion. This motion was experimentally observed in a triaxial TOP trap in Ref. [12]. This periodic solution is best viewed in a frame rotating with the bias magnetic field. In this frame the magnetic moment results in being aligned to the effective magnetic field and the atomic center of mass is at rest. The not-null components of the effective field in the rotating frame, with horizontal component along the x axis, are

$$B_x^{inst} = br \quad \text{and} \quad B_z^{inst} = -2bz + \omega_T s/\mu, \qquad (8)$$

the z component including the uniform fictious magnetic field which appears in the rotating frame. In order to have a stable motion, as produced by a confining potential energy, the component of the spin along the z axis should be positive. In fact the stability along the z axis, requiring a zero force along this direction, leads to

$$\frac{S_z}{s} = \frac{mg}{2b|\mu|} = \xi. \qquad (9)$$

The centrifugal force balancing the gradient force yields the radius of the micromotion:

$$r = \frac{|\mu|b}{m\omega_T^2}\alpha, \quad \alpha = \sqrt{1 - \xi^2}, \qquad (10)$$

where ξ and α are, respectively, the cosinus and sinus of the angle that the effective field $\mathbf{B}^{inst}$ forms with the z axis. In order to determine the z_{eq} height of the periodic orbit under examination, the following parameters also useful in the subsequent analysis are required:

$$\mathbf{s} = \frac{\omega_T s}{\mu b}, \quad \rho = \frac{B_0}{b}, \qquad (11)$$

ρ being the radius of the circle of death [17] and $\mathbf{s}$ is twice the amount the zero point of the quadrupole field shifts downwards for the effect of the uniform fictitious magnetic field which appears in the rotating frame. In terms of these parameters the equilibrium height z_{eq} can be expressed as

$$z_{\text{eq}} = \frac{\mathbf{s}}{2} - \frac{\xi}{\sqrt{1 - \xi^2}}\left(\frac{B_0 + br}{2b}\right) = \frac{\mathbf{s}}{2} - \frac{\xi}{2}\left(\frac{\rho}{\alpha} + \frac{|\mu|b}{m\omega_T^2}\right). \quad (12)$$

The above analysis suggests that the adiabatic approximation is more rigorous if we refer to $\mathbf{B}^{inst}$ instead of the real magnetic field. Indeed, in the motion described above the adiabatic approximation is completely fulfilled with respect to this field. However, for more general solutions of Eqs. (7) the behavior is different and we must also account for a spin component orthogonal to the local magnetic field. In any case, as will be shown in the numerical simulations, the projection of the magnetic moment along this field is a much better conserved quantity with respect to that along the real field. In Refs. [3,30] the effect of the components perpendicular to the real magnetic field have been examined and it was found that a small misalignment with respect to this field gives rise to a Lorentz-type force. An additional electric-type force is originated by the time average of the fast oscillatory force induced by the spin precession. Both kind of forces, affecting the center-of mass dynamics, are geometric forces because they do not depend on the magnitude of the magnetic field but only on its orientation.

III. FROM A CLASSICAL TO QUANTUM ADIABATIC APPROXIMATION

The gross features of the atomic confinement in a magnetic trap are explained in terms of the adiabatic approxima-

tion. If this is fulfilled—that is, when either strong magnetic fields or slowly varying in space fields are involved—the projection $s\sigma$ of the magnetic moment along the direction of the magnetic field is an adiabatic invariant approximatively conserved. The analysis of the previous section points out that an improvement over the standard adiabatic approximation is obtained by replacing the field **B** with **B**^{inst}. Thus, from Eq. (1) we obtain the adiabatic Hamiltonian to be

$$H_{ad}^{\sigma} = \frac{\mathbf{p}^2}{2m} + U_{ad}, \qquad (13)$$

where

$$U_{ad} = mgz + \sigma|\mu|\left[(bx + B_0\cos \omega_T t)^2 + (by + B_0\sin \omega_T t)^2\right.$$

$$\left. + \left(-2bz + \frac{\omega_T s}{\mu}\right)^2\right]^{1/2}. \qquad (14)$$

For small displacements of the atoms from the equilibrium position $(0,0,h)$, the adiabatic potential U_{ad} can be expanded in a power series of the displacement coordinates $(x,y,\zeta=z-z_{eq})$, and up to the second order we have

$$U_{ad}^{(2)} = +mg\left(1 + \frac{\sigma\eta}{\beta\xi}\right)\zeta + \frac{1}{2}m[\omega_{0,r}^2(x^2 + y^2) + \omega_{0,z}^2\zeta^2]$$

$$+ U_0 + U(t). \qquad (15)$$

Here the time-independent component is

$$U_0 = mgz_{eq} + \sigma\beta|\mu|B_0 \qquad (16)$$

and the time-dependent component is

$$U(t,\sigma) = \frac{\sigma|\mu|b}{\beta}\left(1 - \frac{2\eta}{\beta^2}\frac{\zeta}{\rho}\right)(x\cos\omega_T t + y\sin\omega_T t) - \frac{\sigma|\mu|b}{4\rho\beta^3}[(x^2$$

$$- y^2)\cos(2\omega_T t) + 2xy\sin(2\omega_T t)]. \qquad (17)$$

The new adimensional constants here introduced are

$$\eta = \frac{2z_{eq} - s}{\rho}, \quad \beta = \sqrt{1 + \eta^2},$$

while the oscillation frequencies are

$$\omega_{0,r} = \sqrt{\frac{\sigma|\mu|b(2\eta^2 + 1)}{2m\rho\beta^3}}, \quad \omega_{0,z} = \sqrt{\frac{4\sigma|\mu|b}{m\rho\beta^3}}. \qquad (18)$$

Two time scales are involved in $U_{ad}^{(2)}$, the slower one being associated with the harmonic motion at the oscillation frequencies $\omega_{0,r}$ and $\omega_{0,z}$, whereas the faster one is associated with the bias frequency ω_T. The oscillating forces have vanishing time averages over a period $2\pi/\omega_T$. This can be substantiated by the wave function factorization

$$\Psi(\mathbf{x},t,\sigma) = \Phi(\mathbf{x},t,\sigma)\mathcal{E}(\mathbf{x},t,\sigma), \qquad (19)$$

where

$$\mathcal{E} = \exp[-iw/\hbar] \qquad (20)$$

and $w = \int_0^t dt\, U(t,\sigma)$ describes the dominant effects of the oscillating potential. The time-scale separation allows us to

consider $\Phi(\mathbf{x},t)$ as a slowly varying function of time [31]. Notice the explicit dependence on the parameter σ. Substituting Eq. (19) into the Schrödinger equation with the potential $U_{ad}^{(2)}$, we get

$$i\hbar\partial_t\Phi(\mathbf{x},t,\sigma) = \left[\frac{\mathbf{p}^2}{2m} + U_0 + \left(mg + \frac{\sigma\eta}{\beta\xi}\right)\zeta + \frac{1}{2}m[\omega_{0,r}^2(x^2 + y^2)\right.$$

$$\left. + \omega_{0,z}^2\zeta^2]\right]\Phi(\mathbf{x},t,\sigma) + \left[\frac{i\hbar}{m}\boldsymbol{\nabla}w\cdot\boldsymbol{\nabla}\right.$$

$$+ \frac{1}{2m}|\boldsymbol{\nabla}w|^2$$

$$\left. + \frac{i\hbar}{2m}\nabla^2 w\right]\Phi(\mathbf{x},t,\sigma). \qquad (21)$$

The above assumptions on the different time scales allow us to consider the coefficients of the oscillating terms at frequencies ω_T and $2\omega_T$ as slowly varying ones. Indeed a time average over the short time $2\pi/\omega_T$ leads to

$$i\hbar\partial_t\Phi(\mathbf{x},t,\sigma) = \left\{\frac{\mathbf{p}^2}{2m} + mg\left(1 + \frac{\sigma\eta}{\beta\xi} - \frac{\sigma^2\eta}{2\rho\beta^4\xi^2}\frac{g}{\omega_T^2}\right)\zeta\right.$$

$$\left. + \frac{1}{2}m[\omega_r^2(x^2 + y^2) + \omega_z^2\zeta^2]\right\}\Phi(\mathbf{x},t), \quad (22)$$

where the irrelevant constant terms have been dropped. This equation displays a three-dimensional harmonic oscillator structure whose frequences are

$$\omega_r = \omega_{0,r}\left[1 + \frac{\sigma}{16\xi\beta^3}\frac{g}{\rho\omega_T^2}\frac{(32\eta^2 + 1)}{(2\eta^2 + 1)}\right]^{1/2},$$

$$\omega_z = \omega_{0,z}\left[1 + \frac{\sigma}{2\beta^3}\frac{g}{\rho\omega_T^2}\eta^2\right]^{1/2}, \qquad (23)$$

in the xy plane and along the z direction, respectively. The equilibrium position along the z axis is obtained by setting to zero the term multiplying ζ in Eq. (22) . Neglecting smaller contributions, the equilibrium atomic position is given by

$$z_{eq}(\sigma) = s/2 - \rho\xi/(2\sqrt{\sigma^2 - \xi^2}). \qquad (24)$$

In the limit $\sigma=1$ the classical solution of Eq. (12) up to a small term containing ω_T^{-2} is matched. The expectation value of the particle momentum **p** on the state (19) is

$$\langle\mathbf{p}\rangle = \frac{|\mu|b\sqrt{\sigma^2 - \xi^2}}{\omega_T}(-\sin \omega_T t, \cos \omega_T t, 0). \qquad (25)$$

This result is only in part equivalent to the classical one of Eq. (12) because here the instantaneous position value $\langle\mathbf{x}\rangle$ is always zero.

IV. QUANTUM DYNAMICS

A. Effective Hamiltonian

The quantum dynamics is more properly addressed by transforming the original equations into a spin reference

frame rotating at the bias field frequency. Thus the wave function $|\Psi^R\rangle$ in the rotating frame is written as $|\Psi^R\rangle = R_z(-\omega_T t)|\Psi\rangle = \exp[(i/\hbar)s_z\omega_T t]|\Psi\rangle$, where $R_z(\vartheta)$ is the rotation around the z axis by an angle ϑ and $|\Psi\rangle$ is the laboratory frame wave function. Then the Schrödinger equation for $|\Psi^R\rangle$ becomes

$$i\hbar\partial_t|\Psi^R\rangle = i\hbar\partial_t R_z(-\omega_T t)|\Psi\rangle = [H'(t) - \hbar\omega_T s_z]|\Psi^R\rangle$$
$$= H^R|\Psi^R\rangle, \qquad (26)$$

where $H'(t) = R_z(-\omega_T t)H(t)R_z(\omega_T t)$ is time dependent and

$$H^R = H'(t) - \hbar\omega_T s_z = \frac{\mathbf{p}^2}{2m} + mgz - \frac{\mu}{s}\mathbf{s}\cdot\mathbf{B}^R(\mathbf{x},t), \quad (27)$$

with $\mathbf{B}^R(\mathbf{x},t) = [B_0 + b(x\cos\omega_T t + y\sin\omega_T t)]\hat{x} + b(y\cos\omega_T t - x\sin\omega_T t)\hat{y} + (-2bz + \omega_T s/\mu)\hat{z}$. Here $\mathbf{B}^R$ is the magnetic field in the spin-rotating frame, a constant bias field, and a rotating inhomogeneous field. This effective magnetic field $\mathbf{B}^R(\mathbf{x},t) = B_x^R\hat{x} + B_y^R\hat{y} + B_z^R\hat{z}$ identifies the position-dependent angles ϑ and φ as

$$\vartheta = \arctan\frac{\sqrt{(B_x^R)^2 + (B_y^R)^2}}{B_z^R}, \quad \varphi = \arctan\frac{B_y^R}{B_x^R}, \qquad (28)$$

and $B^R = \sqrt{(B_x^R)^2 + (B_y^R)^2 + (B_z^R)^2}$.

B. Local basis

It is useful to introduce a coordinate-dependent spin basis $\{|\chi_m(\mathbf{x},t)\rangle\}$ such that

$$\frac{\mathbf{s}\cdot\mathbf{B}^R(\mathbf{x},t)}{B^R}|\chi_m(\mathbf{x},t)\rangle = m|\chi_m(\mathbf{x},t)\rangle \quad \text{for} -j \leqslant m \leqslant j.$$
$$(29)$$

The local basis vectors in which the z axis coincides with the magnetic field in the same point can be given in terms of the angles ϑ and φ through the rotation operator $M(\varphi,\vartheta)$ as

$$|\chi_m(\vartheta,\varphi)\rangle = M(\varphi,\vartheta)|j,k\rangle = e^{-(i/\hbar)\varphi s_z}e^{-(i/\hbar)\vartheta s_y}|j,k\rangle. \quad (30)$$

With the total wave function expanded as $|\Psi^R\rangle = \sum_{m=-j}^{j}\psi^m(\mathbf{x},t)|\chi_m(\mathbf{x},t)\rangle$, the Hamiltonian of Eq. (27) becomes

$$H^R = \frac{\mathbf{p}^2}{2m} + mgz - \frac{\mu}{s}B^R(\mathbf{x})s_z + \frac{1}{2m}\{2\mathbf{A}\cdot\mathbf{p} + \mathbf{p}(\mathbf{A}) + \mathbf{A}^2\} + \mathcal{V},$$
$$(31)$$

with

$$\mathbf{A} = -(s_z\cos\vartheta - s_x\sin\vartheta)\boldsymbol{\nabla}\varphi - s_y\boldsymbol{\nabla}\vartheta,$$

$$\mathcal{V} = -(s_z\cos\vartheta - s_x\sin\vartheta)\partial_t\varphi - s_y\partial_t\vartheta. \qquad (32)$$

Appendix A contains details useful to derive the functions in Eq. (32). $\mathbf{A}$ and $\mathcal{V}$ represent pseudopotentials connected to the Lorentz-like and electriclike kinds of forces introduced in Ref. [3]. Similar pseudopotentials were derived in [5] as nonadiabatic corrections. The functions $\varphi(\mathbf{x},t)$ and $\vartheta(\mathbf{x},t)$ depend on the effective magnetic field geometry as stated in

Eqs. (28). Berry's geometric terms appear in the quantum Hamiltonian through these angles. By direct computation the following relations are derived:

$$\boldsymbol{\nabla}\vartheta = \frac{[\mathbf{B}^R\times(\mathbf{B}^R\times\boldsymbol{\nabla}\mathbf{B}^R)]_z}{(B^R)^2\sqrt{(B^R)^2 - (B_z^R)^2}}, \quad \boldsymbol{\nabla}\varphi = \frac{[\mathbf{B}^R\times\boldsymbol{\nabla}\mathbf{B}^R]_z}{(B^R)^2 - (B_z^R)^2},$$

$$\partial_t\vartheta = \frac{[\mathbf{B}^R\times(\mathbf{B}^R\times\partial_t\mathbf{B}^R)]_z}{(B^R)^2\sqrt{(B^R)^2 - (B_z^R)^2}}, \quad \partial_t\varphi = \frac{[\mathbf{B}^R\times\partial_t\mathbf{B}^R]_z}{(B^R)^2 - (B_z^R)^2}.$$
$$(33)$$

These terms, invariant with the modulus of the magnetic field, are geometric fields depending only on the force lines of the magnetic field—i.e., the field geometry. Their explicit form is given in Appendix B.

Notice that, starting from the Hamiltonian (1), which is linear in the spin operators, the nonadiabatic terms give rise to a dynamics with a quadratic dependence in the spins. We may write H^R in a form that puts this in more evidence,

$$H^R = \frac{\mathbf{p}^2}{2m} + mgz + \sum_i h^i s_i + \sum_{jk} g^{jk}s_j s_k, \qquad (34)$$

where the indices (i,j,k) run on (x,y,z), and the spin coefficients are

$$h^x = \frac{1}{2m}[\mathbf{p}\sin\vartheta\boldsymbol{\nabla}\varphi + \sin\vartheta\boldsymbol{\nabla}\varphi\mathbf{p}] + \sin\vartheta\partial_t\varphi,$$

$$h^y = -\frac{1}{2m}[\mathbf{p}\boldsymbol{\nabla}\vartheta + \boldsymbol{\nabla}\vartheta\mathbf{p}] - \partial_t\vartheta,$$

$$h^z = -\frac{\mu}{s}B^R - \frac{1}{2m}[\mathbf{p}\cos\vartheta\boldsymbol{\nabla}\varphi + \cos\vartheta\boldsymbol{\nabla}\varphi\mathbf{p}] - \cos\vartheta\partial_t\varphi,$$

$$g^{xx} = \frac{1}{2m}\sin^2\vartheta|\boldsymbol{\nabla}\varphi|^2,$$

$$g^{yy} = \frac{1}{2m}|\boldsymbol{\nabla}\vartheta|^2,$$

$$g^{zz} = \frac{1}{2m}\cos^2\vartheta|\boldsymbol{\nabla}\varphi|^2,$$

$$g^{xz} = g^{zx} = -\frac{1}{2m}\sin\vartheta\cos\vartheta|\boldsymbol{\nabla}\varphi|^2, \qquad (35)$$

and $g^{jk} = 0$ otherwise. Let us recall that all the operators h_i, g_{jk} are Hermitian ones.

V. BEYOND THE ADIABATIC APPROXIMATION

A. Effective spin dynamics

Since the exact solution of the Schrödinger equation (26) is an impracticable task, the dynamics will be taken into account in an effective way by resorting to the TDVP [15]

and by exploiting the time-scale separation between fast and slow degrees of freedom. The TDVP procedure allows us to reduce the system quantum dynamics to a semiclassical Hamiltonian form. This procedure was introduced for studying the low-lying collective states in nuclei, but was later shown to provide a valid approximation also for the one particle Schrödinger equation. Within this procedure, whose details are shown in Appendix C, we choose a suitable trial state of the form

$$\psi(\mathbf{x},t) = \exp[-i\mathcal{S}(t)/\hbar]\Psi(\mathbf{x},t)|j,\tau(t)\rangle, \qquad (36)$$

which will be subjected to the weaker form of the Schrödinger equation embodied into TDVP—i.e., Eq. (C1) in Appendix C. Here $\Psi(\mathbf{x},t)$ and $|j,\tau(t)\rangle$ take in account for the center-of-mass motion and spin dynamics, respectively. $\mathcal{S}(t)$ is an effective action for the spin variables. By carrying out the variational procedure on the trial wave function we derive the classical equations of motion for the expectation values of the spin operators s_j on the spin component of the dynamical trial state $|j,\tau(t)\rangle$. A key point in this variational procedure is the parametrization of the spin variables in terms of coherent atomic states. These latter have the physical significance of angular momentum states produced by a classical source [32]. They depend on a complex parameter τ and are defined as

$$|j,\tau\rangle = \frac{1}{[1+|\tau|^2]^j} \sum_{m=-j}^{j} \left[\binom{2j}{(j+m)} \right]^{1/2} \tau^{j+m}|j,m\rangle, \quad (37)$$

where $|j,n\rangle$ are the spin basis with the quantization axis taken along the direction of the local field. These states, analogous to the coherent states of the electromagnetic field, are defined within a subspace determined by the angular momentum j. Within this subspace each state, completely defined by the complex number τ, is mapped onto the direction of a vector on a sphere by a projective transformation [15]. In our case this vector identifies the orientation of a classical spin with respect to a local frame having the z axis along the local magnetic field $\mathbf{B}^R(\mathbf{x},t)$. This property can be understood by computing the expectation values of the spin components on $|j,\tau\rangle$. By keeping in mind the parametrization $\tau = -e^{-i\varphi'} \tan(\vartheta'/2)$ we find

$$\mathcal{S}_x = \langle j,\tau|s_x|j,\tau\rangle = j\hbar \sin\vartheta' \cos\varphi',$$

$$\mathcal{S}_y = \langle j,\tau|s_y|j,\tau\rangle = j\hbar \sin\vartheta' \sin\varphi',$$

$$\mathcal{S}_z = \langle j,\tau|s_z|j,\tau\rangle = j\hbar \cos\vartheta'. \qquad (38)$$

where ϑ' and φ' are the angles between the classical spin and the local magnetic field. The details of the spin dynamics derivation are contained in Appendix C. Their ruling equations are generated by the classical Hamiltonian of Eq. (C4).

Let us focus on the center-of-mass motion described by the wave function $\Psi(\mathbf{x},t)$ as in Eq. (19) . The trapping potential obtained by the application of TDVP procedure as from Eq. (C2) can be expanded in a power series of the displacement coordinates around the trap center by keeping only the harmonic terms. In this respect we recall that the

center-of-mass dynamics, which will depend on the longitudinal spin component, has the slowest time scale in the system,—i.e., $t_h \approx 2\pi/\omega_{z,r}$—whereas the fastest time scale corresponds to the transverse spin dynamics driven at the Larmor frequency ω_L. Indeed $S_z(t)$—i.e., the longitudinal spin component—is an approximatively conserved adiabatic invariant. For this reason we can assume the center-of-mass motion to be sensitive not just to the instantaneous value of $S_z(t)$ but rather to its time average on a time t intermediate between t_h and $t_L = 2\pi/\omega_L$ which we name $s\,\sigma$. Thus we have

$$\sigma(t) = \frac{\langle S_z \rangle}{s}, \qquad (39)$$

where $\langle S_z \rangle$ stands for the above time average. This coincides with the definition previously introduced within the adiabatic approximation assumption. Since the evolution of this quantity is much slower than the bias frequency $\omega_T(\omega_z \ll \omega_T)$, its time dependence is maintained in the ruling equations even after averaging over the short time scale of the bias-field time-dependent terms as done in order to arrive to Eq. (22) . As a consequence the wave function solution of Eq. (22) can be written as

$$\Phi(\mathbf{x},t,\sigma) = \sum_{\{\mathbf{n}\}} c_{\mathbf{n}}\mathcal{E}_{\mathbf{n}}(t)\Phi_{\mathbf{n}}(\mathbf{x},\sigma), \qquad (40)$$

where the vector index means $\mathbf{n} = (n_1,n_2,n_3)$ along the three orthogonal directions and the constants $c_{\mathbf{n}}$ are determined by the atomic initial conditions. The functions $\Phi_{\mathbf{n}}(\mathbf{x},\sigma)$ are the eigenfunctions of the three-dimensional harmonic oscillator with eigenvalues

$$E_{\mathbf{n}}(\sigma) = U_0 + \frac{1}{2m}\left(\frac{\sigma\mu b}{\beta\omega_T}\right)^2 + \hbar\omega_r(\sigma)(n_1+n_2+1) + \hbar\omega_z(\sigma)$$

$$\times\left(n_3 + \frac{1}{2}\right), \qquad (41)$$

and $\mathcal{E}_{\mathbf{n}}(t) = \exp[i\gamma_{\mathbf{n}}(t)/\hbar - i\int_0^t dt E_{\mathbf{n}}(\sigma(t))/\hbar]$ embodies also a geometric phase

$$\gamma_{\mathbf{n}}(t) = i\hbar \int_{\sigma(0)}^{\sigma(t)} d\sigma\left[\int d\mathbf{x}\,\bar{\Phi}_{\mathbf{n}}(\mathbf{x},\sigma)\frac{\partial}{\partial\sigma}\Phi_{\mathbf{n}}(\mathbf{x},\sigma)\right]. \quad (42)$$

The parameter $\sigma(t)$ entering into the equations of motion for the atomic center of mass is actually a dynamical degree of freedom whose evolution is generated by the classical spin dynamics. Thus, the center-of-mass motion and the spin dynamics interact the one with the other and they must be simultaneously integrated. Let us stress that the dynamics we have just found is the classical canonical counterpart of that one generated by the full quantum Hamiltonian written in Eq. (34).

B. Ground-state configuration

In order to find the nonadiabatic corrections to the ground-state solution (1), we assume that this solution is well represented also if we keep the lowest order in the expression of the Hamiltonian of Eq. (C4)—i.e., the first order in

$(x/\rho, y/\rho, \zeta/\rho)$ appearing in H^R. This means that the Hamiltonian parameters of Eq. (C4), the classical form of Eq. (34), can be computed as an average on the adiabaticlike ground-state solution of Eq. (19) of the approximated operators h^i, g^{jk}. Therefore at the lowest order of approximation the terms in Eq. (35) result:

$$h^x \simeq \frac{1}{m\rho\beta}[-\sin(\omega_T t)p_x + \cos(\omega_T t)p_y],$$

$$h^y \simeq -\frac{1}{m\rho\beta^2}\{\eta[\cos(\omega_T t)p_x + \sin(\omega_T t)p_y] + 2p_z\},$$

$$h^z \simeq -\frac{\mu b\rho}{s}\beta - \frac{\eta}{m\rho\beta}[-\sin(\omega_T t)p_x + \cos(\omega_T t)p_y],$$

$$g^{xx} \simeq \frac{1}{2m\rho^2\beta^2},$$

$$g^{yy} \simeq \frac{3+\beta^2}{2m\rho^2\beta^4},$$

$$g^{zz} \simeq \frac{\eta^2}{2m\rho^2\beta^2},$$

$$g^{xz} \simeq -\frac{\eta}{2m\rho^2\beta^2}.$$

Recalling the expectation value of the momentum $\mathbf{p}$ given by Eq. (25) and neglecting the terms containing $1/\rho^2$, we have

$$\langle h^x_{(0)} \rangle \simeq \frac{2\beta}{\eta(1+2\eta^2)} \frac{\omega^2_{0,r}}{\omega_T},$$

$$\langle h^z_{(0)} \rangle \simeq -\beta \frac{\mu B_0}{s} - \frac{2\beta}{(1+2\eta^2)} \frac{\omega^2_{0,r}}{\omega_T},$$

and 0 otherwise. The corresponding classical spin Hamiltonian is, apart from a constant,

$$\mathcal{H}(\mathcal{S}_x, \mathcal{S}_y, \mathcal{S}_z) = \langle h^x_{(0)} \rangle \mathcal{S}_x + \langle h^z_{(0)} \rangle \mathcal{S}_z,$$

whose equations of motion result:

$$\dot{\mathcal{S}}_x = -\langle h^z_{(0)} \rangle \mathcal{S}_y,$$

$$\dot{\mathcal{S}}_y = -\langle h^x_{(0)} \rangle \mathcal{S}_z + \langle h^z_{(0)} \rangle \mathcal{S}_x,$$

$$\dot{\mathcal{S}}_z = \langle h^x_{(0)} \rangle \mathcal{S}_y. \tag{43}$$

By setting $\dot{\mathcal{S}}_i = 0$ with $(i=x,y,z)$ we determine the ground-state configuration

$$(\mathcal{S}^0_x, \mathcal{S}^0_y, \mathcal{S}^0_z) = \left(\pm \frac{\langle h^x_{(0)} \rangle}{\langle h^z_{(0)} \rangle} \frac{\hbar j}{\sqrt{1 + \langle h^x_{(0)} \rangle^2/\langle h^z_{(0)} \rangle^2}}, 0, \right.$$

$$\left. \pm \frac{\hbar j}{\sqrt{1 + \langle h^x_{(0)} \rangle^2/\langle h^z_{(0)} \rangle^2}} \right). \tag{44}$$

It is worth remarking on the fact that $\langle h^x_{(0)} \rangle$ and $\langle h^z_{(0)} \rangle$ still depend on $\sigma = S^0_z/s$, and thus Eq. (44) determines such a quantity only in a self-consistent way. We point out that in the above equations the plus sign corresponds to the stable solution for the atomic motion in a similar fashion as in the classical description corresponding to Eq. (9). The $\mathbf{S}^0$ solution, with the spin aligned to the local magnetic field, provides a correction to the adiabatic approximation discussed before. We notice that a component $\mathcal{S}^0_x$ different from zero appears because in the rotating frame the rf field acts along the x axis.

C. Effective classical dynamics

The center-of-mass motion is described by the wave function $\Psi(\mathbf{x},t) = \Phi(\mathbf{x},t,\sigma)\mathcal{E}(\mathbf{x},t,\sigma)$ introduced in Eq. (36). The exponential factor $\mathcal{E}(\mathbf{x},t,\sigma)$ has been defined in Eq. (20) and $\Phi(\mathbf{x},t,\sigma)$ satisfies the time-dependent Schrödinger equation (22) for the three-dimensional harmonic oscillator the Hamiltonian of which is $H = \mathbf{p}^2/(2m) + U_h(\mathbf{x}, \sigma(t))$. In terms of the frequencies (23) and of the equilibrium atomic position (24), the time-dependent harmonic potential has the form $U_h(\mathbf{x}, \sigma(t)) = m\{\omega^2_r(\sigma(t))(x^2+y^2) + \omega^2_z(\sigma(t))[z-z_{eq}(\sigma(t))]^2\}/2$.

Upon introducing the center-of-mass position $\mathbf{R} = \langle \Psi|\mathbf{x}|\Psi \rangle$ and momentum $\mathbf{P} = \langle \Psi|\mathbf{p}|\Psi \rangle$, the following classical equations of motion are easily derived:

$$\frac{d\mathbf{R}}{dt} = \frac{\mathbf{P}}{m},$$

$$\frac{d\mathbf{P}}{dt} = -\boldsymbol{\nabla}_{\mathbf{R}}U_h(\mathbf{R}, \sigma(t)) - \frac{d\Delta\mathbf{P}}{dt}, \tag{45}$$

where $\Delta\mathbf{P} = \int d\mathbf{x}|\Phi(\mathbf{x},t)|^2 \boldsymbol{\nabla} w(\mathbf{x},t)$ and $\sigma(t)$ is defined by Eq. (39). Now we introduce a further factorization of the kind $\langle \Psi|\mathcal{O}(\mathbf{x},t)\mathbf{p}|\Psi \rangle \approx \mathcal{O}(\mathbf{R},t)\mathbf{P}$, where $\mathcal{O}(\mathbf{x},t)\mathbf{p}$ stands for the first three among the operators appearing into Eqs. (35) expanded in a power series of $\mathbf{x}$ and $\mathbf{p}$ up to second order [33]. Then by considering only the linear terms in spin variables appearing into the classical spin Hamiltonian (C4) we can write

$$\mathcal{H}(\mathcal{S}_x, \mathcal{S}_y, \mathcal{S}_z) = \sum_i \langle h^i \rangle \mathcal{S}_i, \tag{46}$$

where the time-dependent coefficients are implicit in the center-of-mass wave function $\Psi(\mathbf{x},t)$ as given in Eq. (C5). Thus in Appendix C we derive the following equation of motion for the classical spin:

$$\frac{d\mathcal{S}}{dt} = \mathcal{B}(t) \times \mathcal{S}. \tag{47}$$

where the magnetic field $\mathcal{B}$ is the sum of the real one plus some fictitious terms having originated from the geometric forces with components

$$\mathcal{B}_x(t) = \frac{\left\{ \mathbf{B}^R \times \left[\left(\frac{\mathbf{P}}{m} \cdot \boldsymbol{\nabla} + \partial_t \right) \mathbf{B}^R \right] \right\}_z}{B^R \sqrt{(B_x^R)^2 + (B_y^R)^2}},$$

$$\mathcal{B}_y(t) = -\frac{\left\{ \mathbf{B}^R \times \left[\mathbf{B}^R \times \left[\left(\frac{\mathbf{P}}{m} \cdot \boldsymbol{\nabla} + \partial_t \right) \mathbf{B}^R \right] \right] \right\}_z}{(B^R)^2 \sqrt{(B_x^R)^2 + (B_y^R)^2}},$$

$$\mathcal{B}_z(t) = -\frac{\mu}{s} B^R - \frac{B_z^R \left\{ \mathbf{B}^R \times \left[\left(\frac{\mathbf{P}}{m} \cdot \boldsymbol{\nabla} + \partial_t \right) \mathbf{B}^R \right] \right\}_z}{B^R [(B_x^R)^2 + (B_y^R)^2]}.$$

$$\tag{48}$$

Thus, the two equation systems (45) and (47) form a closed system to be simultaneously integrated.

VI. NUMERICAL SIMULATIONS

We have numerically integrated the set of equations (45) and (47) by means of a Runge-Kutta algorithm. The set of parameters chosen—i.e., $B_0 = 4 \times 10^{-5}$ T, $b = 0.18$ T/m, and $\omega_T = 2\pi \times 10^4$ s^{-1}—correspond to those used in TOP experiments exploring the rubidium micromotion [12,13], but we supposed $s = 1/2\hbar$. The simulations allowed us to recover the atomic micromotion, representing periodic closed orbits. The micromotion was investigated through the classical equations of motion (7) and also through the improved system of equations (45) and (47). Similar results were obtained for the center-of-mass motion. In both approaches we observed a strong dependence on the initial conditions, which for the classical center-of-mass variables are given by Eqs. (24) and (25). For the spin variable the classical condition corresponds to the spin aligned along the local $\mathbf{B}^{inst}$ magnetic field, while the quantum-mechanical solution requires the atom to be in an eigenstate of the spin operator along the local magnetic field. A modification of the initial conditions from those required for the atomic micromotion—for instance, a shift of 100 μm along the z axis—produced the open trajectories shown in Fig. 2. We noticed also a strong dependence on the initial condition for the atomic spin. We also verified that within the parameters used here the correction to the adiabatic approximation expressed by Eq. (44) is not quite relevant. We verified numerically that the spin projection along the effective magnetic field $\mathbf{B}^{inst}$ given by Eq. (8) is well conserved while the spin projection along the real magnetic field $\mathbf{B}$ evidences time-dependent oscillations, as already stated by Ref. [11].

We have explored also a different region of parameter values, where we expect the adiabatic approximation to break down. While the adiabaticity condition is certainly not
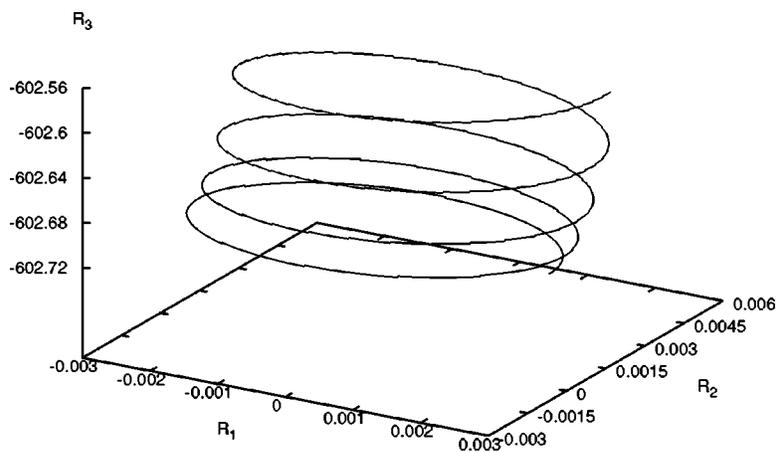
FIG. 2. Plot of a three-dimensional trajectory originated by initial conditions close to those corresponding to the micromotion. The numbers on the axes express the coordinates in μm. This trajectory corresponds to 5 times the $2\pi/\omega_T$ period. It is not closed, while a stable micromotion orbit corresponds to a closed motion. The number on the axes express the coordinates in μm.

fulfilled when $\omega_T \sim \omega_L$, our working assumptions, based on $\omega_z, \omega_r \ll \omega_L$, still hold. A further source of failure for the adiabatic approximation comes for an intensity of the geometric magnetic fields of Eqs. (48) being of the same order of magnitude of the applied real ones. This occurs, for example, at bias field intensities of the order of $B_0 = 2 \times 10^{-7}$ T. Notice that for this weak rotating rf field, the trap oscillation frequencies of Eq. (18) are large enough to sustain the atoms against gravity. However the radius ρ of the circle of death of Eq. (11) becomes comparable to the radius r of the micromotion orbit. Figures 3(a)–3(c) show the components of $\mathcal{B}$ as a function of time obtained with initial conditions very close to those of a micromotion orbit. For this set of parameters it is interesting to make a comparison between the atom dynamics generated by the classical equation of motion and the effective improved equations of motion. The latter give rise to a stable motion, shown in Fig. 3(d) traced by integrating the effective equations (45) and (47). Under the same initial conditions the classical equations of motion generate an unstable trajectory with the atoms conserving initially a constant height $z = 0.73$ μm and then after several milliseconds escaping from the trap. The more stable character of the effective equations solution in respect to the classical ones is made evident by comparing the spin projection along $\mathbf{B}^{inst}$ in both cases. By numerically integrating the effective equations (45) and (47), we found oscillations of $\mathcal{S} \cdot \mathbf{B}^{inst}/|\mathbf{S}||\mathbf{B}^{inst}|$ near the stable value 1. On the contrary, by integrating the classical equations (7), we found a spin flip that causes the condensate escape from the trap. The important role played by the terms originated by the nonadiabatic approximation appears very clearly when we compared the atomic equilibrium within the TOP z_{eq} as derived by the classical solution to that predicted by the effective equations (45) and (47). That comparison is shown in Fig. 4 for a fixed quadrupole field $b = 0.18$ T/m and a rf rotating field B_0 between 1 $\times 10^{-4}$ T and 2×10^{-7} T. At large B_0 the values z_{eq} predicted by the classical solution and the improved one coincide. In-
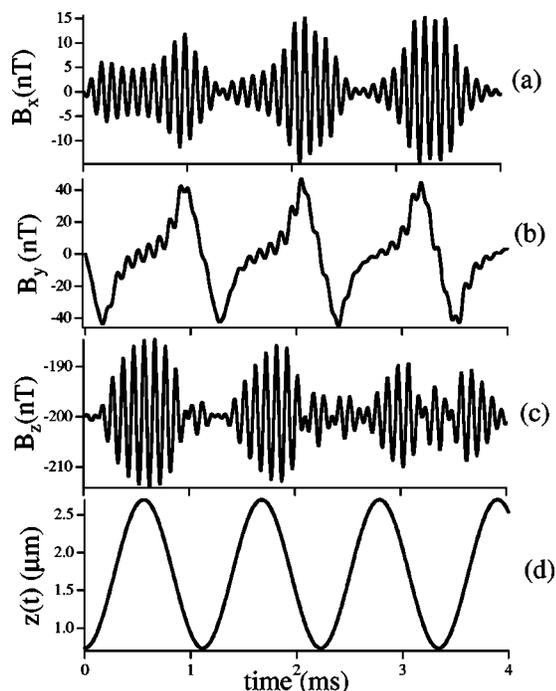
FIG. 3. In (a), (b), and (c) plots of the $\mathcal{B}_x$, $\mathcal{B}_y$, and $\mathcal{B}_z$ geometric fields, in units of $1. \times 10^{-9}$ T, as a function of time in ms for atomic motion within a TOP trap with a rf bias field of 200 nT. In (d) the z position, in μm, of the atomic center of mass traced by integrating the effective equations (45). Instead the integration of the classical equations of motion (7) displays an unstable trajectory.

stead the two values are different at small values of B_0 because the two solutions predict different equilibrium positions. Finally, for $B_0 \approx 5 \times 10^{-7}$ T, classically the atoms, even if suspended against gravity, perform an unstable orbit, sensitive to a minimum spin misalignement from the effective magnetic field. Instead the effective equations predict a stable equilibrium position.

VII. CONCLUSIONS

In this paper we have analyzed the motion of neutral atoms within TOP magnetic traps. We have considered the
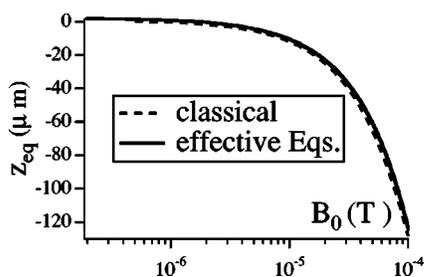
FIG. 4. Comparison between the equilibrium positions z_{eq} of rubidium atoms within the TOP trap versus the B_0 RF field as predicted by the classical solution and by the effective equations (45) and (47) at a given value of the quadrupole field gradient b $=0.18$ T/m. For $B_0 \le 5.0 \times 10^{-5}$ T, the classical model does not support micromotion like orbits.

approximate classical equations of motion describing such system and revisited the fast degrees of freedom motion at the forcing frequency ω_T known as atomic micromotion. In such a motion nonadiabatic effects and geometric fields are absent. Within the scenario of adiabatic approximation, we have analyzed the atomic quantum motion by taking into account the lowest-frequencies terms embodied in the time-dependent potential. Within this approximation, the center-of-mass motion resulting harmonic, we have calculated the harmonic trapping frequencies and recovered the quantum counterpart of the classical micromotion. We have addressed the problem also within a pure quantum context, with a separation of the atomic variables of the spin and of the external degrees of freedom once again based on their different time scales. Within this quantum context, as a consequence of the presence of inhomogeneous magnetic fields geometric magnetic fields appear quite naturally. These geometric fields are responsible for a misalignment of the atomic spin with respect to the local magnetic field and then for nonadiabatic effects. Within this framework, we have derived an effective classical dynamics in which these geometric fields are explicitly embodied. The atomic motion results by the coupling of a quantum harmonic motion, governing the center of mass, and an effective nonlinear spin dynamics driven by both the local magnetic field and the geometric ones.

The numerical simulations performed for the parameters of standard experimental setups have shown that the adiabatic approximation is well suited. On the other hand, by reducing the intensity of the bias field, nonadiabatic effects show up, because the geometric field becomes more relevant and causes misalignment of the spins around $\mathbf{B}^{inst}$. The range of magnetic fields required for the observation of the nonadiabatic effects is experimentally accessible by applying a compensation to the static and alternate spurious external fields.

Another relevant facet concerns the sensitivity to the initial condition of the trap equations. The projection of the atomic magnetic moment of the local field $\mathbf{B}^{inst}$ is a conserved quantity, an adiabatic integral. The initial condition of $\mathbf{S} \cdot \mathbf{B}^{inst}$ chosen for a given simulation identifies a given dynamical evolution, its value remaining conserved during atomic motion. On the other hand, the equilibrium height is determined by the value of this quantity [see Eq. (24)], so that the projection of the atomic magnetic moment on the local field determines the cloud equilibrium height. Now, it is a fact that, for a given geometry of magnetic fields within a trap, such a height results in being independent of the initial preparation condition. Thus, since the dynamical equations do not select by itself any special value of this quantity, one could argue, in order to explain some experimental features of the Bose-Einstein condensate clouds [12,13], which a possible modification of the actual spin projection on $\mathbf{B}^{inst}$ might by involved in some steps of the preparation of the relative Bose-Einstein condensate.

Further attention should also be devoted to the nonlinear interaction within the condensate. In that respect a spinorial Gross-Pitaevskii equation should be solved, and then the analysis applied in Ref. [16] could be used.

APPENDIX A: ABOUT THE su(2) ALGEBRA

The su(2) algebra is defined starting from the angular momentum generators s_x, s_y, s_z and their commutation relations. Using the standard definitions for the raising and lowering operators, we derive the following relations for the derivatives of the operator $M(\phi, \theta)$ defined in Eq. (30):

$$M^\dagger(\varphi, \vartheta)\partial_\varphi M(\varphi, \vartheta) = -\frac{i}{\hbar}(s_z \cos \vartheta - s_x \sin \vartheta),$$

$$M^\dagger(\varphi, \vartheta)\partial_\vartheta M(\varphi, \vartheta) = -\frac{i}{\hbar}s_y,$$

$$M^\dagger(\varphi, \vartheta)\partial_{\varphi\varphi}^2 M(\varphi, \vartheta) = -\frac{1}{\hbar^2}(s_z \cos \vartheta - s_x \sin \vartheta)^2,$$

$$M^\dagger(\varphi, \vartheta)\partial_{\vartheta\vartheta}^2 M(\varphi, \vartheta) = -\frac{1}{\hbar^2}s_y^2,$$

$$M^\dagger(\varphi, \vartheta)\partial_{\varphi\vartheta}^2 M(\varphi, \vartheta) = -\frac{1}{\hbar^2}(s_z \cos \vartheta - s_x \sin \vartheta)s_y,$$

$$M^\dagger(\varphi, \vartheta)s_x M(\varphi, \vartheta) = s_x \cos \vartheta \cos \varphi - s_y \sin \varphi$$
$$+ s_z \sin \vartheta \cos \varphi,$$

$$M^\dagger(\varphi, \vartheta)s_y M(\varphi, \vartheta) = s_x \cos \vartheta \sin \varphi + s_y \cos \varphi$$
$$+ s_z \sin \vartheta \sin \varphi. \tag{A1}$$

APPENDIX B: GEOMETRIC TERMS

For a cylindric TOP trap with magnetic field as defined in Eq. (5), the geometric fields result:

$$\nabla \vartheta = \frac{b}{(B^R)^2\sqrt{(B_x^R)^2+(B_y^R)^2}}\begin{bmatrix} B_z^R\ b(x + \rho \cos \omega_T t) \\ B_z^R\ b(y + \rho \sin \omega_T t) \\ 2[(B_x^R)^2+(B_y^R)^2] \end{bmatrix},$$

$$\nabla \varphi = \frac{b^2}{(B_x^R)^2+(B_y^R)^2}\begin{bmatrix} -y - \rho \sin \omega_T t \\ x + \rho \cos \omega_T t \\ 0 \end{bmatrix},$$

$$\partial_t \vartheta = \frac{\omega_T b^2 B_z^R}{(B^R)^2\sqrt{(B_x^R)^2+(B_y^R)^2}}\rho(y \cos \omega_T t - x \sin \omega_T t),$$

$$\partial_t \varphi = \omega_T\left(\frac{b\rho B_x^R}{(B_x^R)^2+(B_y^R)^2} - 1\right),$$

$$\Delta \vartheta = \frac{B_z^R}{\sqrt{(B_x^R)^2+(B_y^R)^2}}\left(1 + 6\frac{(B_x^R)^2+(B_y^R)^2}{(B^R)^2}\right),$$

$$\nabla \varphi \nabla \vartheta = 0, \quad \Delta \varphi = 0. \tag{B1}$$

APPENDIX C: TDVP APPROACH

In our contest the TDVP method structures the dynamical quantum state describing the atomic motion, in terms of a trial state written, as in Eq. (36), as the product of a time-dependent phase factor $e^{-iS(t)/\hbar}$ times a spatial- and time-dependent scalar wave function $\Psi(\mathbf{x}, t)$ times a time-dependent spinor $|j, \tau(t)\rangle$. The time-dependent trial state $\psi(\mathbf{x}, t)$ has to be found in a self-consisting way. By imposing the weaker form of the Schrödinger equation

$$\int d\mathbf{x}\psi^\dagger(\mathbf{x}, t)[i\hbar\partial_t - H^R]\psi(\mathbf{x}, t) = 0, \tag{C1}$$

we get the effective action $S(t)$:

$$S(t) = \int_0^t dt \int d\mathbf{x}\langle j, \tau(t)|\Psi^\dagger(\mathbf{x}, t)[i\hbar\partial_t - H^R]\Psi(\mathbf{x}, t)|j, \tau(t)\rangle.$$

By splitting the Hamiltonian as $H^R = H_{ad}^\sigma + \Delta H^\sigma$, where H_{ad}^σ has been introduced in Eq. (13), we get

$$S(t) = \int_0^t dt \int d\mathbf{x}\Psi^\dagger(\mathbf{x}, t)[i\hbar\partial_t - H_{ad}^\sigma]\Psi(\mathbf{x}, t)$$
$$+ \int_0^t dt \int d\mathbf{x}\langle j, \tau(t)|[i\hbar|\Psi(\mathbf{x}, t)|^2\partial_t$$
$$- \Psi^\dagger(\mathbf{x}, t)\Delta H^\sigma\Psi(\mathbf{x}, t)]|j, \tau(t)\rangle. \tag{C2}$$

Here $\sigma(t)$ is the slow time-dependent quantity introduced in Eq. (39), which varies on times of the order of $t_h = 2\pi/\omega_{r,z} \gg t_L = 2\pi/\omega_L$. By expanding the Hamiltonian H_{ad}^σ in a power series of the displacement coordinates $(x, y, \zeta = z - h)$, we get the harmonic Hamiltonian with the time-dependent potential of Eq. (15). Thus, by introducing the structure $\Psi(\mathbf{x}, t)$ of Eq. (19) for the atomic wave function we find the Schrödinger equation (21). After taking the time average of the latter equation on a short time $2\pi/\omega_T$, we get the harmonic problem (22) of which the general solution $\Phi(\mathbf{x}, t)$ is known. Thus, the first term on the right-hand side in Eq. (C2) vanishes, and we obtain

$$S(t) = \int_0^t dt\langle j, \tau(t)|[i\hbar\partial_t - \langle\Delta H_{(2)}^\sigma\rangle]|j, \tau(t)\rangle,$$

where $\langle\Delta H_{(2)}^\sigma\rangle = \int d\mathbf{x}[\Psi^\dagger(\mathbf{x}, t)\Delta H_{(2)}^\sigma\Psi(\mathbf{x}, t)]$ and $\Delta H_{(2)}^\sigma$ is obtained by expanding ΔH^σ in a power series in $\mathbf{x}$ and $\mathbf{p}$ up to the second order. Explicitly we have

$$\langle \Delta H_{(2)}^{\sigma} \rangle = \sum_i \langle h_{(2)}^i \rangle s_i + \sum_{jk} \langle g_{(2)}^{jk} \rangle s_j s_k - \langle \sigma \mu B_{(2)}^{R} \rangle,$$

with the obvious meaning of index (2).

The Hamiltonian $\langle \Delta H_{(2)}^{\sigma} \rangle$ is built of su(2) algebra generators acting on the time-dependent spin vector $|j, \tau(t)\rangle$. We choose for $|j, \tau(t)\rangle$ the components of the su(2) atomic coherent state $|\tau(t)\rangle$ of j representation. As a support for this choice let us remember that, if the Hamiltonian $\langle \Delta H_{(2)}^{\sigma} \rangle$ was a closed dynamical algebra—i.e., a linear combination of the su(2) generators—the solutions of the Schrödinger equation given by these coherent states would be exact [15]. The equation of motion for the label $\tau(t)$ (and its complex conjugate), which involves the dynamical evolution of the state $\psi(\mathbf{x}, t)$, is obtained by stationarizing the effective action $S(t)$:

$$\delta S = \delta \left(\int_0^t dt \left\{ i\hbar \, \langle j, \tau(t) | \left[\dot{\tau} \frac{d}{d\tau} + \dot{\overline{\tau}} \frac{d}{d\overline{\tau}} \right] | j, \tau(t)\rangle - \langle j, \tau(t) \right. \right.$$

$$\left. \left. \times | \rangle \Delta H_{(2)}^{\sigma} \rangle \Big| j, \tau(t) \right\rangle \right) = 0. \tag{C3}$$

After boring algebra we get the equations of motion

$$\frac{d\tau}{dt} = \frac{(1 + |\tau|^2)^2}{2i\hbar j} \partial_{\overline{\tau}} \mathcal{H}(\tau, \overline{\tau}),$$

where $\mathcal{H}(\tau, \overline{\tau}) = \langle \tau | \Delta H_{(2)}^{\sigma} | \tau \rangle$ and $\overline{\tau}$ is the complex conjugate of τ. These tricky equations can be cast in more familiar form

by writing them in terms of the classical spin components $\mathcal{S}_x, \mathcal{S}_y, \mathcal{S}_z$ introduced in the text. The dynamics of these spin components, apart terms irrelevant for the equations of motion, is generated by the following Hamiltonian:

$$\mathcal{H}(\mathcal{S}_x, \mathcal{S}_y, \mathcal{S}_z) = \sum_i \langle h_{(2)}^i \rangle \mathcal{S}_i + \left(1 - \frac{1}{2j} \right) \sum_i \langle g_{(2)}^{ii} \rangle \mathcal{S}_i^2 + 2 \left(1 - \frac{1}{2j} \right)$$

$$\times \langle g_{(2)}^{xz} \rangle \mathcal{S}_x \mathcal{S}_z, \tag{C4}$$

where the time-dependent coefficients are derived by the center-of-mass wave function $\Psi(\mathbf{x}, t)$ as

$$\langle h_{(2)}^i \rangle = \int d\mathbf{x} [\Psi^{\dagger}(\mathbf{x}, t) h_{(2)}^i \Psi(\mathbf{x}, t)] \quad \text{for} \quad i = x, y, z,$$

$$\langle g_{(2)}^{ij} \rangle = \int d\mathbf{x} [\Psi^{\dagger}(\mathbf{x}, t) g_{(2)}^{ij} \Psi(\mathbf{x}, t)] \quad \text{for} \quad i, j = x, y, z, \tag{C5}$$

and the operators h^i and g^{ij} have been given in Eq. (35) . Therefore we obtain a canonical system for the classical spin components whose dynamics is generated by the effective Hamiltonian $\mathcal{H}$, endowed with the Poisson brackets $\{\mathcal{S}_x, \mathcal{S}_y\} = \mathcal{S}_z$ and cyclic permutations.

[1] For an introduction see the supplement in J. J. Sakurai, *Modern Quantum Mechanics* (Addison-Wesley, Boston, 1994). For a review see A. Shapere and F. Wilczek, *Geometric Phases in Physics* (World Scientific, Singapore, 1989). For a list of experiments on Berry's phase see J. Anandan, J. Christiam, and K. Wakelik, Am. J. Phys. **65**, 180 (1997).

[2] An early study of the nonadiabatic processes for the atomic motion within an inhomogeneous magnetic field was made by E. Majorana, Nuovo Cimento **9**, 44 (1932).

[3] Y. Aharonov and A. Stern, Phys. Rev. Lett. **69**, 3593 (1992).

[4] An additional velocity-dependent potential is derived in R. G. Littlejohn and S. Weigert, Phys. Rev. A **48**, 924 (1993).

[5] C.-P. Sun, M.-L. Ge, and Q. Xiao, Commun. Theor. Phys. **13**, 63 (1990); C.-P. Sun and M.-L. Ge, Phys. Rev. D **41**, 1349 (1990).

[6] T.-L. Ho and V. B. Shenoy, Phys. Rev. Lett. **77**, 2595 (1996).

[7] C. V. Sukumar and D. M. Brink, Phys. Rev. A **56**, 2451 (1997).

[8] E. A. Hinds and C. Eberlein, Phys. Rev. A **61**, 033614 (2000).

[9] R. M. Potvliege and V. Zehnlé, Phys. Rev. A **63**, 025601 (2001).

[10] V. I. Yukalov, Phys. Rev. A **56**, 5004 (1997).

[11] J. Schmiedmayer and A. Scrinzi, Quantum Semiclassic. Opt. **8**, 693 (1996); J. R. Anglin and J. Schmiedmayer, Phys. Rev. A **69**, 022111 (2004).

[12] J. H. Müller, O. Morsch, D. Ciampini, M. Anderlini, R. Man-

nella, and E. Arimondo, Phys. Rev. Lett. **85**, 4454 (2000).

[13] J. H. Müller, O. Morsch, D. Ciampini, M. Anderlini, R. Mannella, and E. Arimondo, C. R. Acad. Sci. Paris, **t.2 IV**, 649 (2001).

[14] R. Geursen, N. R. Thomas, and A. C. Wilson, Phys. Rev. A **68**, 043611 (2003).

[15] W. M. Zhang, D. H. Feng, and R. Gilmore, Rev. Mod. Phys. **62**, 867 (1990); T. Fukui and Y. Tsue, Prog. Theor. Phys. **87**, 627 (1992); A. Montorsi and V. Penna, Phys. Rev. B **55**, 8226 (1997).

[16] K. J. Challis, R. J. Ballagh, and C. W. Gardiner, e-print: cond-mat/0406497.

[17] W. Petrich, M. H. Anderson, J. R. Ensher, and E. A. Cornell, Phys. Rev. Lett. **74**, 3352 (1995).

[18] M. H. Anderson, J. R. Ensher, M. R. Matthews, C. E. Wieman, and E. A. Cornell, Science **269**, 198 (1995).

[19] E. W. Hagley, L. Deng, M. Kozuma, J. Wen, K. Helmerson, S. L. Rolston, and W. D. Phillips, Science **283**, 1706 (1999).

[20] D. J. Han, R. H. Wynar, Ph. Courteille, and D. J. Heinzen, Phys. Rev. A **57**, R4114 (1998).

[21] B. P. Anderson and M. A. Kasevich, Phys. Rev. A **59**, R938 (1999).

[22] J. L. Martin, C. R. McKenzie, N. R. Thomas, J. C. Sharpe, D. M. Warrington, P. J. Manson, W. J. Sandle, and A. C. Wilson, J. Phys. B **32**, 3065 (1999).

[23] J. Arlt, O. Maragó, E. Hodby, S. A. Hopkins, G. Hechen-

blaikner, S. Webster, and C. J. Foot, J. Phys. B **32**, 5861 (1999).

[24] The different experimental configurations are characterized by the components of the quadrupole gradients along the orthogonal axes appearing in Eq. (3) and by the plane containing the rotating magnetic field of Eq. (4). The geometry of the Pisa experiment with a triaxial TOP trap corresponds to $-b_x=-b_y=b_z/2=b$ and the B_0 field rotating in the horizontal plane [25].

[25] J. H. Müller, D. Ciampini, O. Morsch, G. Smirne, M. Fazzi, P. Verkerk, F. Fuso, and E. Arimondo, J. Phys. B **33**, 4095 (2000).

[26] V. G. Minogin, J. A. Richmond, and G. I. Opat, Phys. Rev. A **58**, 3138 (1998).

[27] S. Gov and S. Shtrikman, J. Appl. Phys. **86**, 2250 (1999).

[28] D. S. Hall, J. R. Ensher, D. S. Jin, M. R. Matthews, C. E. Wieman, and E. A. Cornell, Proc. SPIE **3270**, 98 (1998).

[29] The factorization of the wave function has been discussed in [10].

[30] M. V. Berry, Proc. R. Soc. London, Ser. A **452**, 1207-1220 (1996).

[31] R. J. Cook, D. G. Shankland, and A. L. Wells, Phys. Rev. A **31**, 564 (1985).

[32] L. Mandel and E. Wolf, *Optical Coherence and Quantum Optics* (Cambridge University, Cambridge, England, 1995).

[33] Since the center-of-mass motion is described by a three-dimensional harmonic oscillator Hamiltonian, the center-of-mass wave function is given at all times by a Glauber coherent state $|\alpha\rangle$ representing the minimum indetermination state [32] . It is easy matter to verify that $\langle\alpha|(xp+px)/2|\alpha\rangle=\langle\alpha|x|\alpha\rangle\langle\alpha|p|\alpha\rangle$. Therefore the factorization applies to those states.